

Vortex Force at Large Angle of Attack and for Long Time

J. Li¹, and Z.N. Wu¹

¹Department of Engineering Mechanics
Tsinghua University, Beijing 100084, China

Abstract

Recently, it was found that the first cycle of time-dependent force oscillation for high angle of attack flow of a flat plate is split into (1) a force enhancement stage due to building and early motion of an LEV (leading edge vortex), (2) a stall stage due to the high upwash effect of an TEV (trailing edge vortex) just built downstream of the trailing edge since this high upwash reduces the pressure below the plate, (3) a force recovery stage during which the force lost in stall is partly recovered due to pressure suction effect of the well-established TEV having moved above rear part of the plate, and (4) a force release stage during which the force recovered is partly released due to blown off of the TEV. A new leading edge vortex is then built and a new cycle of force oscillation starting with force enhancement appears.

In this paper, we consider the time evolution of the force for a very long time, including more periods to study whether the above four stages repeat in time and whether there exist new stages other than these four stages.

1. Introduction

High angle-of-attack (AoA) flows occur in many applications including flapping wings of insects [3] and of micro air vehicles [2], fixed wings of delta shape [8], and turbines undergoing pitching, plunging, heaving during manoeuvring [1]. A large number of studies have been devoted to this problem with the primary concern of vortex shedding and movement, and of the relation of the force in association with the pattern of vortices, using theoretical analysis [4-6,9], experimental measurement [2,7], discrete vortex simulation [5,6,12], or computational fluid dynamics simulations [11]. Once the intensity and velocity of vortices and their rate of production are given by experimental, numerical or theoretical analysis, the force can be related to the rate of production, intensity and velocity of these vortices, through using various equivalent forms of the moment equation for flow, such as the algebraic Bernoulli equation, the unsteady Blasius equation or integral approaches.

It has been found that in large AoA flow, leading edge vortex still close to the leading edge enhances the lift [2]. Apart from force enhancement, the newly created trailing edge vortex due to the approach of detached leading edge vortex either reduces the force (when it is downstream of the trailing edge during its creation) to induce stall or recovers the force lost in stall when it moves above the rear part of the wing [6]. Li & Wu [6] thus decompose the time evolution of force into four repeatable stages: force enhancement, stall, force recovery and force release. But this study only showed the first period of force variation.

In this paper, we consider long time force evolution, with about seven periods of force oscillation, for high AoA flow, majorly for a flat plate but a result for Joukowski airfoil is also displayed.

In section 2, we recall the methods of vortex force analysis (vortex force line map, suction force analogy, upwash force reducing mechanism for stall, and CFD method). In section 3, the results for a flat plate with AoA equal to 45 degree and 60 degree

for both inviscid and viscous flows are considered. In section 4, the results for a Joukowski airfoil are displayed. The main conclusions are summarized in section 5.

2. Methods for Vortex Force Study

In this section, the method for vortex force analysis given by Li & Wu [6] is briefly outlined. The method by Streitlien & Triantafyllou [10] for Joukowski airfoil is also recalled.

2.1. Vortex Force Related to Potential Vortices

Assume at any instant, there are I point vortices, in unsteady flow around a flat plate at high AoA, each with position $x_v^{(i)}, y_v^{(i)}$, $i = 1, 2, \dots, I$, velocity $\vec{V}_v^{(i)} = d(x_v^{(i)}, y_v^{(i)}) / dt$ and circulation $\Gamma_v^{(i)}$ (positive for a counter-rotating vortex). The flat plate of chord length c_A lies over $0 < x < c_A, y = 0$. Li & Wu [6] derived the normal force expression

$$F_y = \rho \sum_{i=1}^I \vec{V}_v^{(i)} \cdot \vec{\Lambda}(p_i, q_i) \Gamma_v^{(i)} \quad (1)$$

where $\vec{\Lambda}(p_i, q_i) = (P, Q)(p_i, q_i)$ is the vortex force factor that depends on the position of the point vortex only. Here

$$\begin{cases} p = (x_v^{(i)} - \frac{1}{2}c_A) / \frac{1}{2}c_A, q = y_v^{(i)} / \frac{1}{2}c_A \\ P(p, q) = 1 - \partial C_1 / \partial p + 2\partial E_1 / \partial p \\ Q(p, q) = -\partial C_1 / \partial q + 2\partial E_1 / \partial q \end{cases} \quad (2)$$

with

$$\begin{cases} C_1 = \frac{1}{\pi} (p(\lambda_0 - \lambda_1) + \lambda_1 - \frac{1}{2}(\lambda_0 + \lambda_2)) \\ E_1 = \frac{1}{4\pi} ((p-1)(\lambda_0 + \lambda_2) + (\frac{3}{2} - 2p)\lambda_1 + \frac{1}{3}\lambda_3) \\ \lambda_n = \int_0^\pi \frac{\cos(n\beta)}{(p + \cos\beta)^2 + q^2} d\beta, x = \frac{1}{2}c_A(1 - \cos\beta) \end{cases} \quad (3)$$

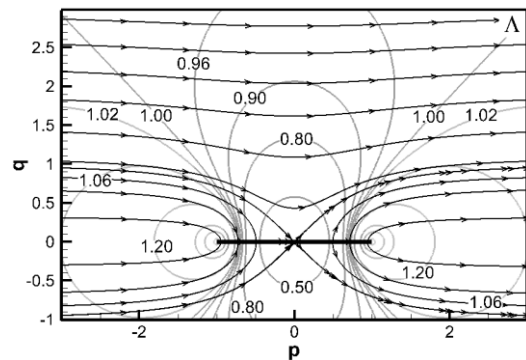


Figure 1. The vortex force line (VFL) map for a flat plate [6]. The curves with arrows are VFLs, similar to stream lines but with the velocity factor

replaced by the vector of vortex force factor. The curves without arrows are contours of the vortex force factor.

Li and Wu [6] used the vortex force factor $\bar{\lambda}(p, q)$ to build a vortex force line map in the plane (p, q) , arrowed force lines are locally parallel to the vector $\bar{\lambda}(p, q)$. See Figure 1. An leading edge vortex with $\Gamma_v^{(i)} < 0$ moving in a direction (called favourable direction) intersecting the arrowed force line at obtuse or acute angle enhances or reduces lift, and the effect is reversed for a trailing edge vortex ($\Gamma_v^{(i)} > 0$).

Li & Wu [6] derived the force for potential vortices but found that the formula holds approximately true for non-potential concentrated vortices, for both inviscid and viscous flow.

For Joukowski airfoil under arbitrary motion and with free vortices in the flow, Streitlien & Triantafyllou [10] gave a general formula of the force, which for an impulsively started or fixed airfoil can be written as, in the complex plane,

$$F_x + iF_y = i \sum_{i=1}^I \Gamma_v^{(i)} \frac{d}{dt} \left(\frac{dz_v^{(i)}}{dt} - \frac{c^2}{\bar{\zeta}_v^{(i)}} - \frac{a^2}{\zeta_v^{(i)} + \zeta_c} \right) \quad (4)$$

Here, $\zeta_v^{(i)}$ is the position of the vortex i in the circle plane and $z_v^{(i)}$ is in the airfoil plane. These two planes are related by the Joukowski transformation

$$z = \zeta + \zeta_c + a^2 / (\zeta + \zeta_c)$$

Here $c = |a - \zeta_c|$ is the radius of the circle and ζ_c is the centre of the circle. We have numerically checked that equation (1) and (4) are equivalent for a flat plate.

2.2. Suction Force and High Upwash Negative Force

The vortex force approach is mathematical and is very hard to be used for clarifying why the force is enhanced or reduced by a given vortex. Li & Wu [6] then used a pressure distribution analysis to study how a concentrated vortex enhances and reduces the force. The various force stages can be explained using figure 2.

a) Force enhancement by pressure suction. An LEV closely above the leading edge causes a suction force on the upper surface of the flat plate. Dickinson & Gotz [2] first proposed this force enhancement mechanism following the delta wing analogy of Polhamus [8]. However, it was long believed that this pressure suction force assumes that the leading edge vortex is attached. In fact, for unsteady flow it never attaches. Pressure suction force exists even the leading edge vortex is moving, provided it is still near and above of the plate.

b) Stall due to high upwash effect. This occurs when a TEV is triggered out by the approach of LEV to the trailing edge. Initially, this TEV is close to and downstream of the trailing edge, so that it induces a high upwash flow below the rear part of the plate. This high upwash reduces greatly the pressure below the rear part of the plate, giving a strong negative force (called high upwash force), which is responsible for stall.

c) Force recovery by pressure suction. The TEV created in the stall stage now moving upstream to above the rear part of the plate causes pressure suction on the upper surface of the trailing edge. This vortex force is similar to the LEV suction analogy, so that the force lost during stall is recovered (TEV suction analogy).

d) Force release by the release of pressure suction. With the TEV blown off away from the rear part of the plate, the TEV suction force is weakened, and the force curve starts to drop.

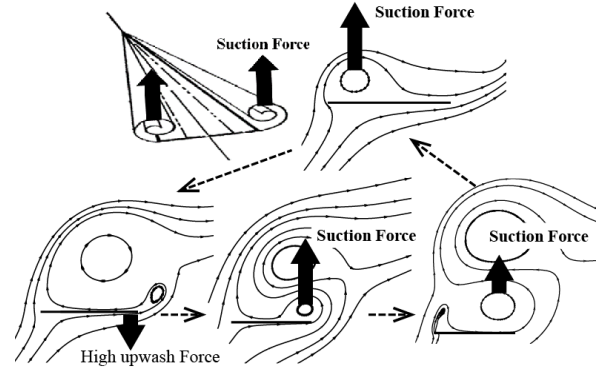


Figure 2. Pressure suction analogy and upwash effect.

After force release a new LEV is built and we get a new force enhancement stage. The other stages should also be repeated as will be checked below through displaying CFD results for long time.

2.3. Numerical Method

We use computational fluid dynamics (CFD) as in Li and Wu [6], we solve the Euler equations for inviscid flow and the Navier–Stokes equations for viscous flow, using the commercial code Fluent with the options of a second-order upwind PISO (pressure implicit with splitting of operators) pressure–velocity coupling method for incompressible flow, with second-order upwind scheme for momentum equation and second-order method for pressure equation. For a flat plate, we use the same grid (200 grid points along each side of the flat plate, refined near the leading and trailing edges) as in Li and Wu [6], and for a Joukowski airfoil, the total grid of the mesh we use is 18121 with 170 grid points along the wall. The Wagner model was used for validation of CFD method.

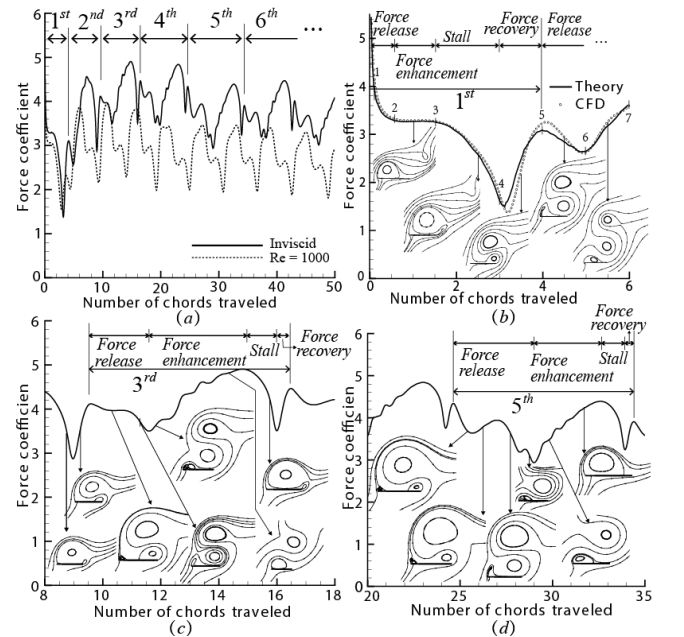


Figure 3. The evolution of normal force for flat plate starting flow with AoA equal to 45 degree: (a) For both inviscid flow and viscous flow with $Re = 1000$, the non-dimensional time up to $\tau = 50$; (b) Force for inviscid flow by means of two methods, and the streamlines of flow field in

typical instants in the first period [6]; (c) Force and streamlines in typical instants in the third period for inviscid flow; (d) Force and streamlines in typical instants in the fifth period for inviscid flow.

3. Flat Plate Flow for Long Time

The force curve (in terms of the non-dimensional force coefficient versus the non-dimensional time $\tau = V_{\infty} t / c_A$) is displayed in figure 3(a). Both inviscid flow and viscous flow (with a Reynolds number 1000) are displayed. The non-dimensional time τ is the number of chords travelled. In the present study we give results for $0 < \tau < 50$ while Li & Wu [6] only displayed the results for $0 < \tau < 6$.

The force curve covers about 7 periods for $0 < \tau < 50$, as can be seen in Figure 3(a). Table 1 displays the periods (the time interval between two peak values of the force coefficient, or time interval between two instants where a leading edge vortex is newly created).

	Cycle No	1	2	3	4	5	6
inviscid	Period	4.1	5.5	6.9	8.1	9.8	8.7
	Max of Cn	NaN	4.56	4.9	4.84	4.39	4.47
	Min of Cn	1.38	2.57	3.51	3.46	2.94	3.17
Re=1000	Period	3.7	4.4	4.9	5.1	5.7	5.7
	Max of Cn	NaN	3.87	3.95	3.82	3.43	3.46
	Min of Cn	2.84	2.01	2.16	2.29	1.98	1.99

Table 1. The period length and maximum/minimum values of force coefficient curve in each period for AoA equals 45 degree.

a) Periods:

For inviscid flow, the first cycle has a period of 4.1 (in terms of the non-dimensional time); the second cycle has a period of 5.5, which is 1.4 larger than the first one. The third cycle has a period of 6.9, which is 1.4 larger than the second cycle. The 4th cycle has a period of 8.1, which is 1.2 larger than the third one. The 5th cycle has a period of 9.8, which is 1.7 larger than the 4th one. The 6th cycle has a period of 8.7, which is 1.1 smaller than the 5th one. The period is increased from the first cycle to the 5th cycle. The flow is not exactly periodical at least for $0 < \tau < 50$. But for very large time, the periods of different cycles are close.

For viscous flow, the first cycle has a period of 3.7 and the second cycle has a period of 4.4, which is 0.7 larger than the first one. The third cycle has a period of 4.9, which is 0.5 larger than the second cycle. The 4th cycle has a period of 5.1, which is only 0.2 larger than the third one. The 5th and the 6th cycle have the same period of 5.7, which is 0.6 larger than the 4th one.

For the series of cycles displayed, viscosity reduces the length of period.

b) Peak values or amplitude:

For inviscid flow, the maximal value of the force coefficient in the first cycle is infinite due to the initial singularity [4] and the minimal value is 1.38. For the second cycle, the maximal value is 4.56 and the minimal value is 2.57. The maximal/minimal values of the third cycle are 4.9/3.51, the maximum is increased slightly and the minimum is increased sharply by nearly 1. For the 4th cycle, the maximal/minimal values reduce to 4.84/3.46. For the 5th cycle, the maximal/minimal values reduce sharply to 4.39/2.94. And for the 6th cycle the maximal/minimal value increase slightly to 4.47/3.17.

For viscous flow, the maximal value in the first cycle is large due to initial singularity [11] and the minimal value is 2.84. For the second cycle, the maximal/ minimal values reduce to 3.87/2.01. The maximal/minimal value of the third cycle increase to 3.95/2.16; For the 4th cycle, the maximal values reduce slightly to 3.82 and the minimal value increase slightly to 2.29. For the 5th cycle, the maximal/minimal values reduce sharply to 3.43/1.98. The maximal/minimal value in the 6th cycle is nearly the same as in the 5th cycle.

Thus, the maximal value for inviscid flow in each period is larger than viscous flow, and the minimal value for inviscid flow is also larger than viscous flow except for the first cycle. For inviscid flow the force oscillation amplitude (the maximal value minus the minimal value) for each period is around 1.4 except for the initial two periods. For viscous flow the amplitude decreases in the first four cycle, and then reaches a relative stable value of approximately 1.5 from the 5th cycle.

c) Force stage in each cycle:

The first cycle has been shown to contain a force release stage, force enhancement stage, stall stage and force recovery stage by Li & Wu [6]. Here, for later cycles, we still observe a force release, enhancement, stall and recovery. See Fig 3(b) for the first cycle, figure 3(c) for the 3rd cycle, and figure 3(d) for the 5th cycle. All exhibit the same variation in association with the leading edge vortex and trailing edge vortex.

During the force release stage, the trailing edge vortex moves off the trailing edge. The force enhancement stage corresponds to the existence of a leading edge vortex near leading edge. Stall occurs when a TEV is right of the trailing edge. Force recovers when this TEV moves above the rear part of the trailing edge. Finally, when this TEV was blown off the force releases.

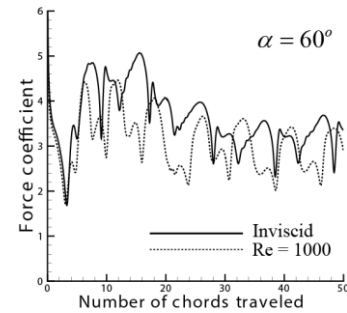


Figure 4. The evolution of force for flat plate at AoA 60 degree.

Figure 4 gives the evolution of the normal force coefficient for flat plate started impulsively at AoA of 60 degree. Table 2 displays the periods and maximum/minimum values of force coefficient curve in each cycle. The results are similar to the case of AoA at 45 degree. The period and the maximum/minimum value for $\alpha = 60^\circ$ are larger than the case of $\alpha = 45^\circ$.

	Cycle No	1	2	3	4	5	6
inviscid	Period	4.4	5.4	8.0	10.9	10.6	9.9
	Max of Cn	NaN	4.85	5.07	4.41	3.56	3.68
	Min of Cn	1.68	3.16	3.51	2.62	2.32	2.42
Re=1000	Period	4.0	4.9	5.9	7.6	7.0	7.8
	Max of Cn	NaN	4.42	4.46	4.06	3.66	3.61
	Min of Cn	1.72	2.41	2.77	2.37	2.14	2.14

Table 2. The period length and maximum/minimum values of force coefficient curve in each period for AoA equals 60 degree.

For up to $\tau = 50$, the period length does not reach a unique value when time grows, though the difference is small after the fourth cycle. There is a great change of the amplitude of force oscillation at the fifth cycle. The force release stage for the first cycle has a monotonic force curve, while for the other cycles, the force curve of the force release stage is not monotonic, due to the existence of LEV and TEV from previous cycles.

Moreover, for the first cycle, force releases from the initial singularity, while for the later cycles, force releases from a finite value built during the recovery stage. For long time, there are additional small-amplitude oscillations caused by the existence of LEVs and TEVs shed previously.

4. Joukowski Airfoil Flow

The results for Joukowski airfoil (thickness 0.2, camber 0.04) started impulsively with the same condition for the flat plate case in section 3 is displayed in figure 5. The results are similar to those of a flat plate, thus the vortex force analysis (including pressure suction and upwash effect) appears to hold true for Joukowski airfoil. Details for this and for more general airfoils will be considered in the future.

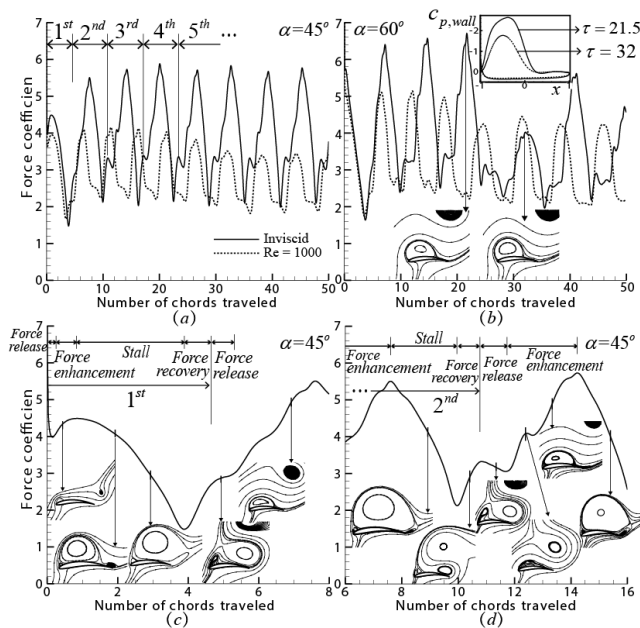


Figure 5. The force evolution for Joukowski airfoil (similar to figure 3).

5. Conclusions

In this paper, we have summarized the main physics of force variation due to alternative shedding of LEV and TEV for high AoA flow and for very long time.

We found that for long time each cycle of force oscillation is still composed of a force release stage, a force enhancement stage, a force stall and a force recovery stage, as for the first cycle studied previously. There are slight variations of the period lengths and oscillation amplitudes. The 2nd to fourth cycles have larger amplitude of oscillation and from the fifth cycle the amplitude of

oscillation is reduced. There are more small amplitude oscillations with respect to the first cycle due to existence of LEVs and TEVs shed previously.

Moreover, the results for a Joukowski airfoil appears to show that the conclusions obtained for a flat plate also hold for an airfoil, thus a theory is required to justify this conclusion.

Acknowledgments

This work was supported by the Natural National Science Foundation of China (No. 11472157) and partly by the National Basic Research Program of China (No. 2012CB720205).

References

- [1] Choudhry, A., Leknys, R., Arjomandi, M. & Kelso, R., An insight into the dynamic stall lift characteristics, *Experimental Thermal and Fluid Sciences*, **58**, 2014, 188–208.
- [2] Dickinson, M.H. & Gotz, K.G., Unsteady aerodynamic performance of model wings at low Reynolds numbers, *Journal of Experimental Biology*, **174**, 1993, 45–64.
- [3] Ellington, C.P., Van Den Berg C., Willmott, A.P. & Thomas, A.L.R., Leading-edge vortices in insect flight, *Nature*, **384**, 1996, 626–630.
- [4] Graham J.M.R., The initial lift on an aerofoil in starting flow, *Journal of Fluid Mechanics*, **133**, 1983, 413–425.
- [5] Li, J. & Wu, Z. N., Unsteady lift for the Wagner problem in the presence of additional leading/trailing edge vortices, *Journal of Fluid Mechanics*, **769**, March, 2015, 182–217.
- [6] Li, J. & Wu, Z. N., A vortex force study for a flat plate at high angle of attack, *Journal of Fluid Mechanics*, **801**, 2016, 222–249.
- [7] Pitt Ford C.W. & Babinsky H., Lift and the leading-edge vortex, *Journal of Fluid Mechanics*, **720**, 2013, 280–313.
- [8] Polhamus E C., A concept of the vortex lift of sharp-edge delta wings based on a leading-edge-suction analogy. 1966.
- [9] Pullin D.I., & Wang Z. J., Unsteady forces on an accelerating plate and application to hovering insect flight. *Journal of Fluid Mechanics*, **509**, 2004, 1–21.
- [10] Streitlien K. & Triantafyllou M.S. Force and moment on a Joukowski profile in the presence of point vortices, *AIAA Journal*, **33**, 1995, 603–610.
- [11] Wang, Z. J., Vortex shedding and frequency selection in flapping flight, *Journal of Fluid Mechanics*. **410**, 2000, 323–341.
- [12] Xia X., & Mohseni K., Lift evaluation of a two-dimensional pitching flat plate, *Physics of Fluids*, **25**(091901), 2013